Developmental Cell
Article

Redefining the Progression of Lineage Segregations during Mammalian Embryogenesis by Clonal Analysis

Elena Tzouanacou,[1,5,*] Amélie Wegener,[1,4] Filip J. Wymeersch,[2] Valerie Wilson,[2,3] and Jean-François Nicolas[1,3]
[1]Institut Pasteur, Département de Biologie du Développement, CNRS URA 2578, 25 rue du Dr. Roux, 75724 Paris cedex 15, France
[2]Institute for Stem Cell Research/MRC Centre for Regenerative Medicine, School of Biological Sciences, University of Edinburgh, University of Edinburgh, King's Buildings, West Mains Rd., Edinburgh EH9 3JQ, UK
[3]These authors contributed equally to this work
[4]Present address: UMR 546 INSERM-UPMC, Hôpital de la Pitié-Salpêtrière, 105 bd de l'hôpital, 75634 Paris cedex 13, France
[5]Present address: Department of Physiology, Development and Neuroscience, University of Cambridge, Downing Street, Cambridge CB2 3DY, UK
*Correspondence: tzouanacou@gmail.com
DOI 10.1016/j.devcel.2009.08.002

SUMMARY

Clonal lineage information is fundamental in revealing cell fate choices. Using genetic single-cell labeling in utero, we investigated lineage segregations during anteroposterior axis formation in mouse. We show that while endoderm and surface ectoderm segregate during gastrulation, neural ectoderm and mesoderm share a common progenitor persisting through all stages of axis elongation. These data challenge the paradigm that the three germ layers, formed by gastrulation, constitute the primary branchpoints in differentiation of the pluripotent epiblast toward tissue-specific precursors. Bipotent neuromesodermal progenitors show self-renewing characteristics and may represent the cellular substrate coupling sustained axial elongation and coordinated differentiation of these tissues. These findings have important implications for the interpretation of the phenotypic defects of several mouse mutants and the directed differentiation of embryonic stem (ES) cells in vitro.

INTRODUCTION

Gastrulation is crucial to the early patterning of bilaterian embryos. During this process, the embryo is not only transformed from a single layer of pluripotent epithelium to a trilayered structure composed of ectoderm, mesoderm, and endoderm, but also the axes of the embryo become apparent. In amniote embryos, the pluripotent epithelium, termed the epiblast (Gardner and Rossant, 1979), produces mesoderm and endoderm via ingression through the primitive streak, while cells remaining in the epiblast give rise to surface ectoderm and neurectoderm (Tam and Behringer, 1997). By the end of gastrulation, only the head and most anterior trunk structures are formed. Elongation of the embryo continues through organogenesis by the supply of cells in the posterior neuropore and later in the tail bud at the caudal end of the embryo (Stern et al., 2006).

Lineage tracing studies in cultured mouse embryos allowed the construction of fate maps delineating the relative positions of progenitor populations in the epiblast/streak and tail bud and indicated a temporal order of cell recruitment to the embryonic tissues that corresponds to the anteroposterior (AP) axis (Cambray and Wilson, 2002, 2007; Tam and Behringer, 1997). Single cell labeling in pre- and early streak embryos showed that despite the apparent regionalization of progenitors, epiblast cells are able to contribute descendants to multiple germ layers, indicating that the primary embryonic lineages have still not segregated at the onset of gastrulation (Lawson et al., 1991; Lawson and Pedersen, 1992). At later stages, in situ labeling and orthotopic grafting of cell groups suggested that elongation of the postcranial axis depends on small progenitor population(s) close to and within the late primitive streak and its descendant, the tail bud (Tam and Beddington, 1987; Wilson and Beddington, 1996). Furthermore, it has been proposed, in both mouse and chick, that at least some of the cells in the anterior streak/node region and later the chordoneural hinge (CNH) of the tail bud constitute one or more stem cell population(s) that persist over the period of axial elongation and give rise to cells in the neural tube, somites, and notochord (Cambray and Wilson, 2002, 2007; McGrew et al., 2008). However, these latter prospective lineage studies are not informative about the fate of single progenitor cells, leaving open the possibility that the cell groups initially labeled were mixed populations of cells, whose fates are restricted to specific tissues and shorter axial segments. At the level of individual cells, retrospective analyses of clonal descendants in either the myotome or central nervous system (CNS) provided conclusive evidence that these tissues derive from stem cell pool(s) (Mathis and Nicolas, 2000; Nicolas et al., 1996). However, the origin of these cells and whether they represent separate tissue-specific progenitors or a single multipotent cell population remain elusive.

Consistent with the possibility that the entire axis is formed by one multipotent or several tissue-specific stem cell pools, the tail bud gives rise to tail tissues in continuity with those in the trunk. However, tail outgrowth does not show the dramatic cell movements of gastrulation, and the neural tube forms by a distinct process in the tail relative to the head and trunk levels (Griffith et al., 1992; Schoenwolf, 1984; Schoenwolf and Delongo, 1980). In addition, several mutations affect posterior axis formation leaving anterior structures intact. These differences led to a long-lasting debate on whether anterior and posterior body are formed by the same or different mechanisms (reviewed in Handrigan, 2003).

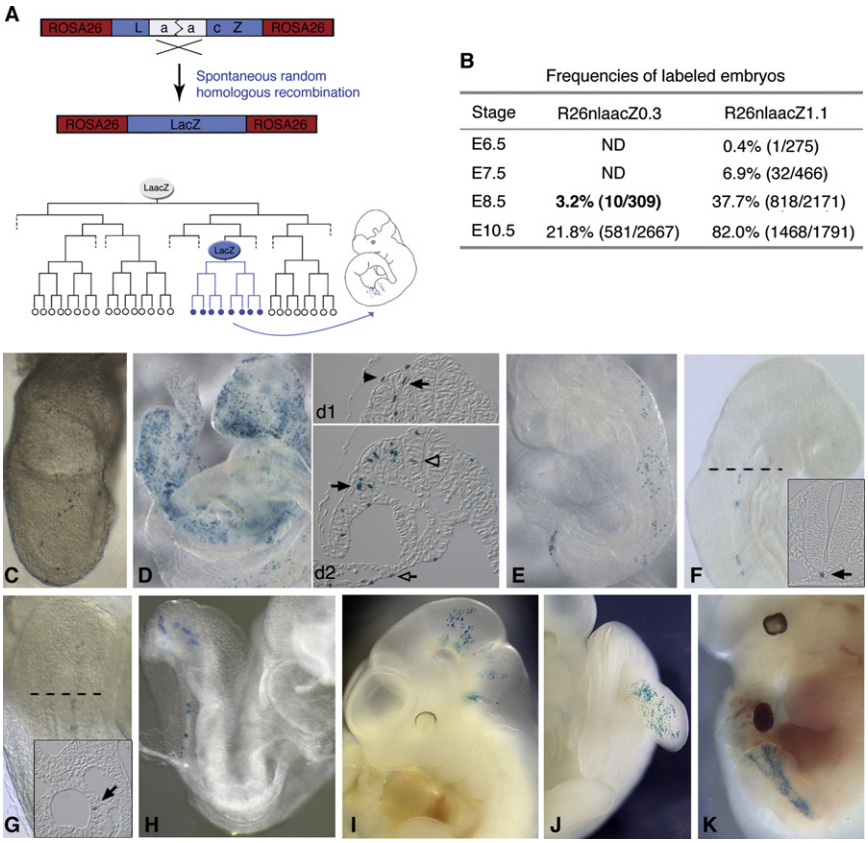

Figure 1. R26nlaacZ Cell Labeling System

(A) Schematic representation of the approach.

(B) The frequency of labeled embryos increases with the size of *laacZ* duplication and the embryonic age. In parentheses, number of heterozygote embryos examined (or homozygotes, in bold); ND, not determined.

(C–K) Examples of clones.

(C) E7.5 mesoderm clone.

(D) E8.5 clone in ectoderm and mesoderm and (d1, d2) sections at mid-trunk level showing labeled nuclei in surface ectoderm (arrowhead, d1), somite (arrow, d1), neural tube (open arrowhead, d2), lateral mesoderm (arrow, d2), yolk sac mesoderm (open arrow, d2).

(E) Long E8.5 surface ectoderm clone.

(F) E8.5 notochord clone; inset, section at the level of the broken line.

(G and H) E8.5 hindgut clones; inset in (G): section at the level of the broken line.

(I) E10.5 midbrain-hindbrain clone.

(J–K) Hindlimb bud clones in E10.5 surface ectoderm (J), and E12.5 mesoderm (K).

Here, we investigate the progression of fate restrictions and cell behavior from gastrulation to tail bud stage at clonal level. We used a genetic method of single cell labeling in utero that allows long-term tracing of all clonal descendants, analyzed retrospectively at different stages during axis formation. This method relies on the spontaneous reversion of a *laacZ* gene, carrying an inactivating sequence duplication, to an active *lacZ* reporter via rare intragenic homologous recombination within the duplication (Bonnerot and Nicolas, 1993).

RESULTS

R26nlaacZ Cell Labeling System

Systematic clonal analyses using *laacZ/lacZ* mosaics were previously performed to investigate cellular patterning of the embryonic muscle, myocardium, CNS, and melanocytes (Eloy-Trinquet and Nicolas, 2002a, 2002b; Mathis and Nicolas, 2000, 2003, 2006; Meilhac et al., 2003, 2004a, 2004b; Nicolas et al., 1996; Wilkie et al., 2002). In these studies, *laacZ* expression was restricted to these domains in the embryo via the use of tissue-specific promoters. Accordingly, labeling of a precursor cell allowed visualization of only a fraction of its progeny allocated to the tissues defined by the specific promoter activity. To trace cell descendants irrespective of their tissue distribution, and thus examine the progression of lineage segregations, we inserted *laacZ* into the ubiquitously expressed Rosa26 locus (Soriano, 1999; Figure 1A).

We generated two mouse lines, *R26nlaacZ0.3* and *R26nlaacZ1.1*, carrying *laacZ* genes with different duplication sizes (289 bp and 1117 bp respectively; see Figure S1A available online). *R26nlacZ* ES cell lines showed infrequent, small clusters of β-galactosidase positive (β-gal$^+$) cells, while all cells of the control *R26nlacZ* line were β-gal$^+$ (Figures S1B and S1C). The rate of *laacZ* recombination, determined by fluctuation analysis in ES cell cultures, was found to be 4.8-fold higher in *R26nlaacZ1.1* line compared to *R26nlaacZ0.3* line (1.7×10^{-6} and 8.1×10^{-6}, respectively), indicating that the rate increases in concert with the duplication size. The frequency of labeled embryos varied accordingly in these two mouse lines and also increased with age, reflecting the increase in the number of cells that can undergo recombination as the embryo grows (Figure 1B). Clones of variable size (number of β-gal$^+$ cells) were detected in all tissues and axial levels of embryos examined at different stages, consistent with the expectation that recombination can occur randomly in any cell during development (Figures 1C–1K).

Probability of *laacZ* Recombination during Embryogenesis in *R26nlaacZ* Mouse Lines

Given that the *laacZ* recombination is a spontaneous and random event, the probability of labeling a precursor cell in an embryo (or within a specific cell population) is directly proportional to the rate of recombination per cell and per generation and the number of cells in the embryo (or cell population) at any given stage. Therefore, a comprehensive representation of the different progenitor populations present in the embryo over time necessitates examination of a large number of embryos and a recombination rate sufficiently high to obtain clones derived even from progenitors present in small numbers, particularly those in embryos at early stages.

As shown in Figure 1B, the frequency of labeled *R26nlaacZ0.3* embryos is very low at early stages (3% in E8.5 homozygotes). In addition, smaller clones, representing recent recombination

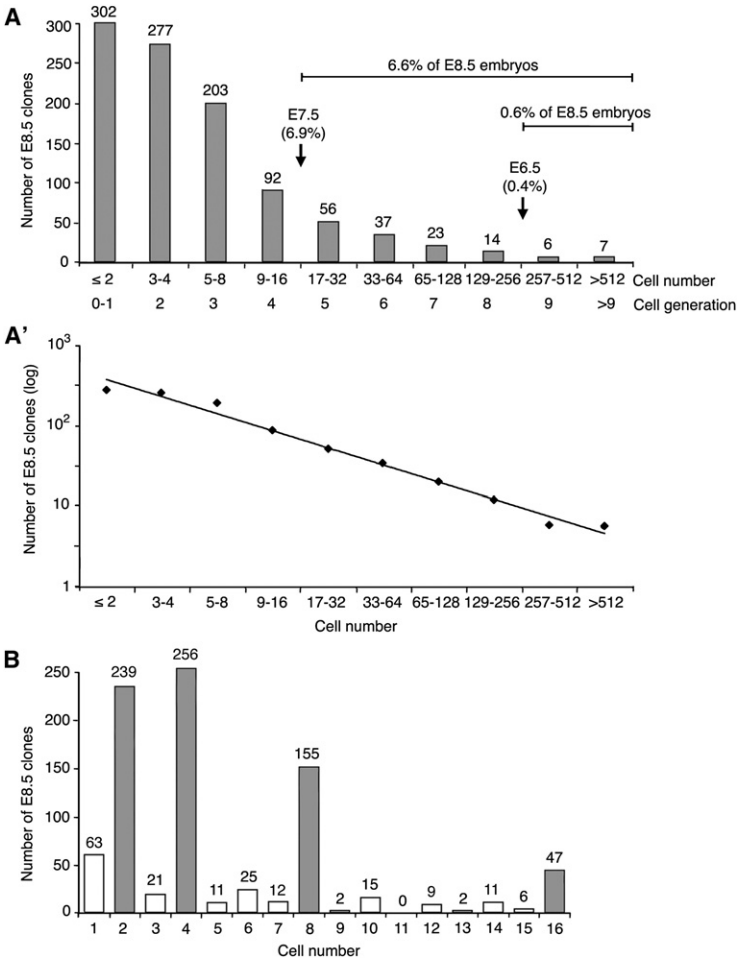

Figure 2. Proliferative Growth and Synchrony in Cell Division during Gastrulation and Early Organogenesis

(A) Number of E8.5 clones with exponentially increasing sizes (β-gal$^+$ cells). The distribution fits an exponential curve (see A′). The frequencies of clones with >16 and >256 cells in E8.5 embryos are similar to the total frequencies of clones in embryos examined at E7.5 and E6.5, respectively. (A′) Fit of log-transformed data in A to a linear regression line ($R^2 = 0.98$, $p < 0.0001$, 8 d.f.).

(B) Number of small clones in relation to their exact cell number. One thousand seventeen clones are represented in (A) and (A′). These correspond to 818 labeled embryos in 2171 total embryos examined. One hundred sixty-eight embryos showed two to four distant clusters that were considered as independent clones (compare with Figure S2, E8.5 R26nlaacZ1.1 x ≥ 1).

events, are as expected more frequent than larger (earlier) clones. Thus, overall, 98% of E8.5 and E10.5 *R26nlaacZ0.3* embryos have ≤4 and ≤30 cells labeled respectively. These findings indicate that the *R26nlaacZ0.3* recombination rate is too low to allow comprehensive analysis of cell behavior prior to early organogenesis, since the vast majority of clones arise after E8.5. In contrast, the higher recombination rate in *R26nlaacZ1.1* allele results in higher frequency of embryos labeled during gastrulation and early organogenesis (Figure 1B; see also Figure 2), making this line more suitable for a systematic clonal analysis during these stages.

Statistical assessment of the clonal relationship of labeled cells in the embryos showed that secondary recombination events may occur in an embryo but such contamination can be easily monitored since it concerns small clones (recent events) that occur with higher frequency (Figure S2; Supplemental Data). In addition, due to the random nature of recombination, independent events are unlikely to occur in the same location within the embryo (Figure S3; Supplemental Data). Therefore, the labeling pattern (tissue distribution and spatial arrangement of β-gal$^+$ cells) in an embryo carrying two clones is unlikely to be similar to the patterns in other embryos. In order to exclude embryos in which more than one clone is present, we based our conclusions regarding common tissue progenitors on embryos where the number of labeled cells in each tissue is higher than that expected for a secondary event, and where a similar pattern of labeled cells was observed in several embryos (Figure S2; Tables S1 and S2).

Embryo Growth during Gastrulation and Early Organogenesis

The onset of gastrulation in mouse is accompanied by an increase in cell proliferation. Cells undergo approximately four divisions in 24 hr, such that the cell number in the embryonic region increases from 660 at E6.5 to approximately 15,000 at E7.5 (Lawson et al., 1991; Snow, 1977). We found that the number of cells in embryos at E8.5 is 1.7 ± 0.2 SEM × 10^5 (see Experimental Procedures), indicating that a high proliferation rate, with an average cell generation time of ~7 hr, is maintained during early organogenesis.

The size distribution of E8.5 clones (Figures 2A and 2A′) indicates that growth is exponential with no major events of withdrawal from the cell cycle during this period. High levels of cell death or existence of postmitotic cell populations would lead to a decrease in the number of progenitors and distort the size distribution. Additionally, small E8.5 clones grouped according to their exact cell number reveal that classes of 4, 8, and 16 cells are overrepresented, implying that there is a certain degree of synchrony in cell division (Figure 2B). This trend is also evident when clones contributing to specific germ layers are considered (data not shown).

Given that growth is exponential up to at least early organogenesis, it is possible to estimate the birth date of clones in E8.5 embryos based on their size and the average growth rate between E6.5 and E8.5 (Figure 2A). According to this calculation, clones with more than 16 cells were initiated prior to late gastrulation and those with more than 256 cells no later than early gastrulation. To exclude the possibility that the generation time varies considerably between cells in distinct lineages, introducing a bias to this estimation, we compared the proportions of E8.5 embryos, presenting clones in these size classes, with the total frequencies of labeled embryos dissected at E6.5 and E7.5 (early and late gastrulation, respectively). We found that these empirically measured frequencies closely match those estimated from the E8.5 clonal size distribution, indicating that our estimation of the clonal birth date is indeed accurate (Figure 2A; see also Figure 1B).

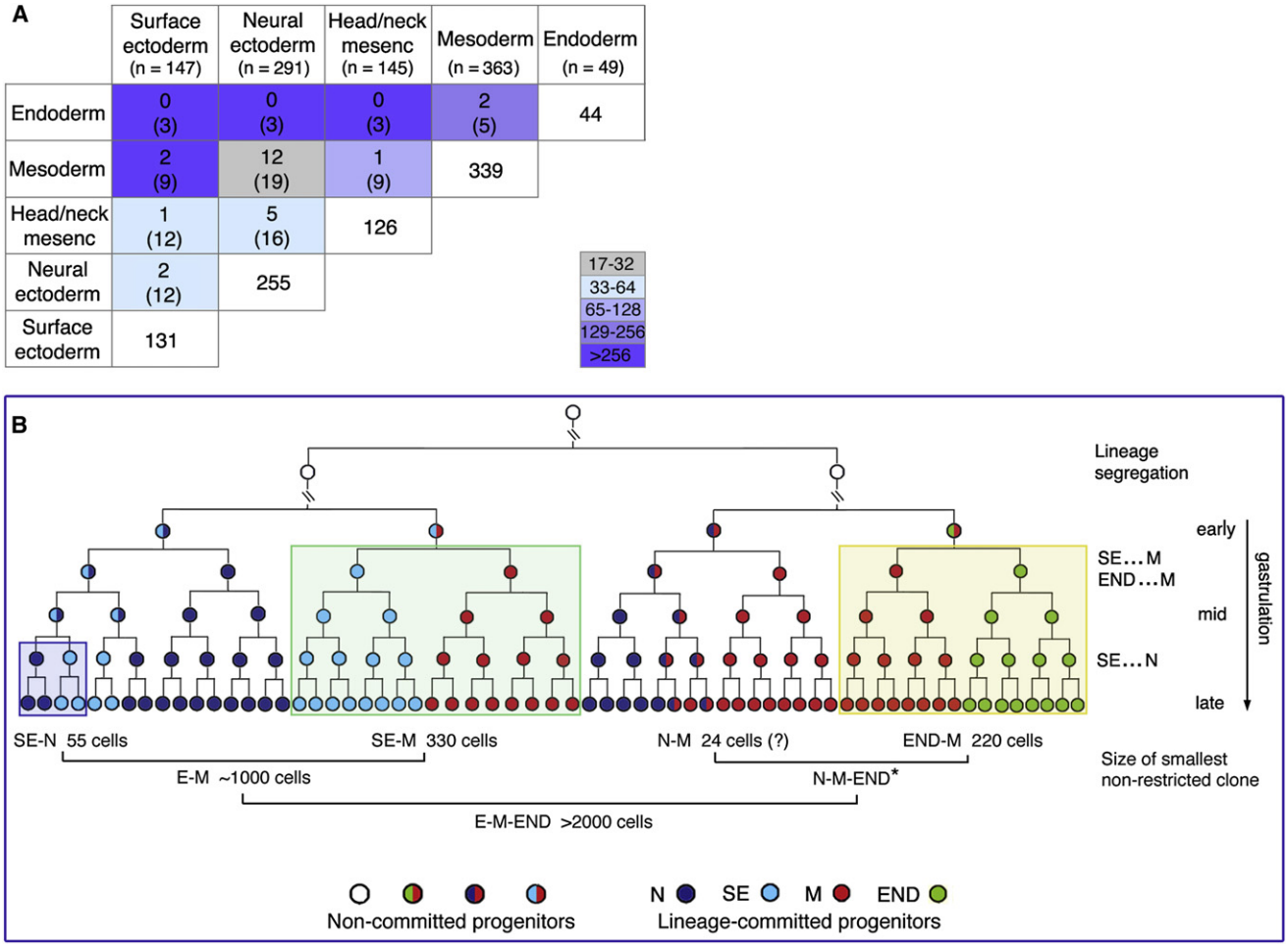

Figure 3. Segregation of Embryonic Lineages Observed in E8.5 Embryos

(A) R26nlaacZ1.1 clones are classified according to the tissue distribution of labeled cells. (n) shows the total number of clones with cells in each tissue. White squares indicate the number of tissue-restricted clones. Colored squares show the number of clones contributing exclusively to the tissue combination indicated by the corresponding row and column headings (top figures) and the total number of clones with cells in this tissue combination (figures in parentheses). The difference between these numbers correspond to clones with contribution to more than two tissues. The size of the smallest clone in each tissue combination is color coded as indicated. Head/neck mesenchyme includes both neural crest and cranial mesoderm.

(B) Schematic representation of the data in (A). The diagram shows the sequence of lineage segregations as indicated by the size of the smallest clone in each tissue/germ-layer combination. It takes into account the relative frequencies of embryos with labeled derivatives in each tissue and the preferential associations of tissue derivatives in the clones. The tissue associations observed in clones initiated during early gastrulation are in agreement with the regionalization of progenitors indicated by the fate maps but do not necessarily imply an inherent difference between cells at this stage (third line of progenitors from the top). The polyclonal origin of embryonic tissues has been ignored for simplicity. E, ectoderm (SE + N); END, endoderm; SE, surface ectoderm; N, neurectoderm; M, mesoderm;. \\ indicates cell generations not shown. N-M-END* corresponds to a single clone with this tissue contribution detected only at E10.5 and extending along the entire AP axis.

Early Segregation of Endoderm and Surface Ectoderm

To examine the progression of lineage segregations, we analyzed the tissue distribution of 1017 clones produced in E8.5 embryos (8–16 somites) with respect to their size. Since initiation of a clone is random, the frequency of a clonal category (clones with contribution to a specific tissue or tissue combination) is proportional to the number of progenitors of that category. Furthermore, the size of the smallest clones not restricted to a single tissue provides information about the stage at which embryonic lineages segregate.

Forty-nine clones, representing 2% of the total embryos examined (see Experimental Procedures), colonize the definitive endoderm (Figure 3A). Of these, only five clones with an estimated birth date prior to or at early gastrulation (>200 cells) contribute descendants to other germ layers. Existing fate maps show that endoderm progenitors are located in a region of the epiblast that also produces cranial and heart mesoderm and they traverse the streak during early gastrulation, concurrently with extraembryonic mesoderm (Lawson et al., 1991). Consistent with these data, the two smallest nonrestricted endoderm clones also colonize these tissues (Figure 4, AW14.4, ET155.1). The three largest clones with endoderm contribution (>1500 cells) show labeled cells in all epiblast-derived tissues and two of these also contribute to the visceral endoderm

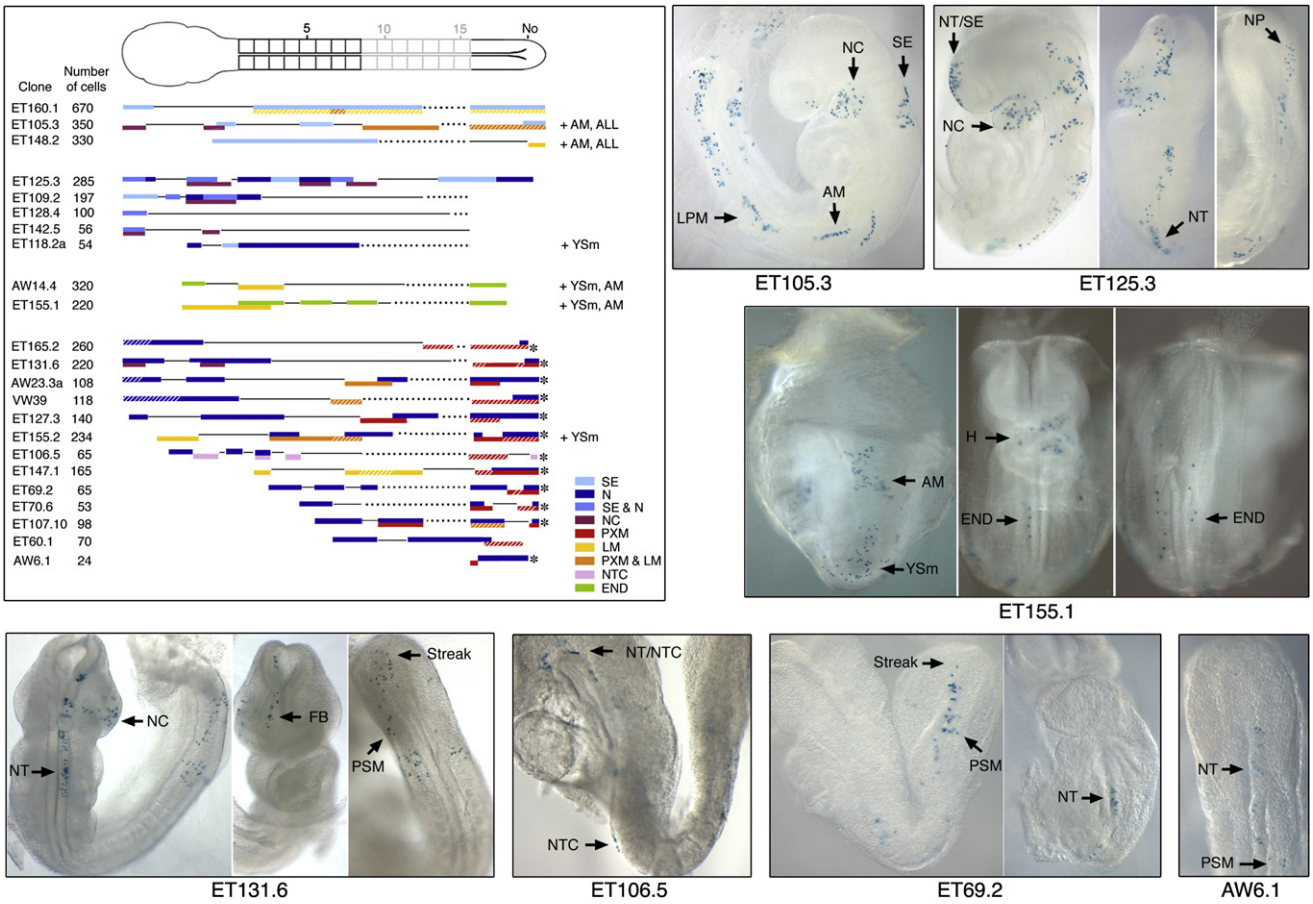

Figure 4. Schematic Representation of Nonrestricted E8.5 Clones and Representative Embryos of Each Clonal Category

Clones in the drawing are grouped by clonal category and within each category ordered by anterior border. Six very large clones contributing to multiple tissues (≥1000 cells) are not shown. Tissue contribution is color-coded as indicated. Hatched blocks represent bilateral contribution; solid lines correspond to unlabeled regions and dotted lines to axial levels not formed (variable region faded in embryo drawing). Contribution to the neuropore posterior to the node is indicated by an asterisk. ALL, allantois; AM, amnion; END, endoderm; FB, forebrain; H, heart; LM, lateral mesoderm; N, neurectoderm; NC, neural crest; NP, neuropore; No, node; NT, neural tube; NTC, notochord; PXM, paraxial mesoderm; PSM, presomitic mesoderm; SE, surface ectoderm; Ysm, Yolk sac mesoderm.

(data not shown). Three additional very large clones (>1000 cells) do not colonize the endoderm even though they have labeled derivatives distributed along the entire AP axis in all other embryonic tissues as well as the extraembryonic mesoderm (Figure 1D and data not shown). The large size of nonrestricted endoderm clones (>200 cells), and the observation that only three of the six largest clones with multiple tissue contribution colonize the endoderm, suggest that endoderm progenitors segregate from other lineages shortly after the onset of gastrulation (Figure 3B).

The total frequency of clones with cells in endoderm (2%, restricted and nonrestricted) was much lower compared to that of clones with contribution to ectoderm (20%) and mesoderm (17%). Assuming a similar recombination rate in all embryonic tissues, this suggests that the overall endoderm precursor pool (committed and noncommitted progenitors) is small. To exclude the possibility that the difference in clonal frequencies is due to a varying recombination rate in differentiating cells, we next considered only nonrestricted clones, derived from progenitors in the early epiblast prior to their commitment to a specific lineage (≥129 cells, n = 18). Comparison of the proportions of nonrestricted clones in ectoderm (16/18), mesoderm (16/18), and endoderm (5/18) indicates that the pool of endoderm progenitors prior to their segregation at early gastrulation is indeed small relative to the other germ layers (Fisher's exact test, p = 2E-04).

Twenty-two of sixty-six clones initiated before late gastrulation (>16 cells), and having labeled cells in ectoderm, also contribute to the embryonic mesoderm. Examination of the ectodermal tissues labeled shows that only very large clones (>300 cells; n = 9) colonize both surface ectoderm and mesoderm, suggesting an early segregation of these lineages (Figures 3A and 3B; Figure 4, ET160.1, ET105.3, ET148.2). Segregation of the ectodermal lineages appears to occur later since the two smallest clones contributing to both surface ectoderm and neurectoderm have approximately 55 cells (Figures 3A and 3B; Figure 4, ET142.5, ET118.2a). The most striking clonal relationship was found between neurectoderm and mesoderm. A large proportion of neurectoderm clones with more than 16 cells (37%; 19/52) also have labeled derivatives in mesoderm (Figure 3A; Figure 4, lower clonal group). Significantly, most of these clones show

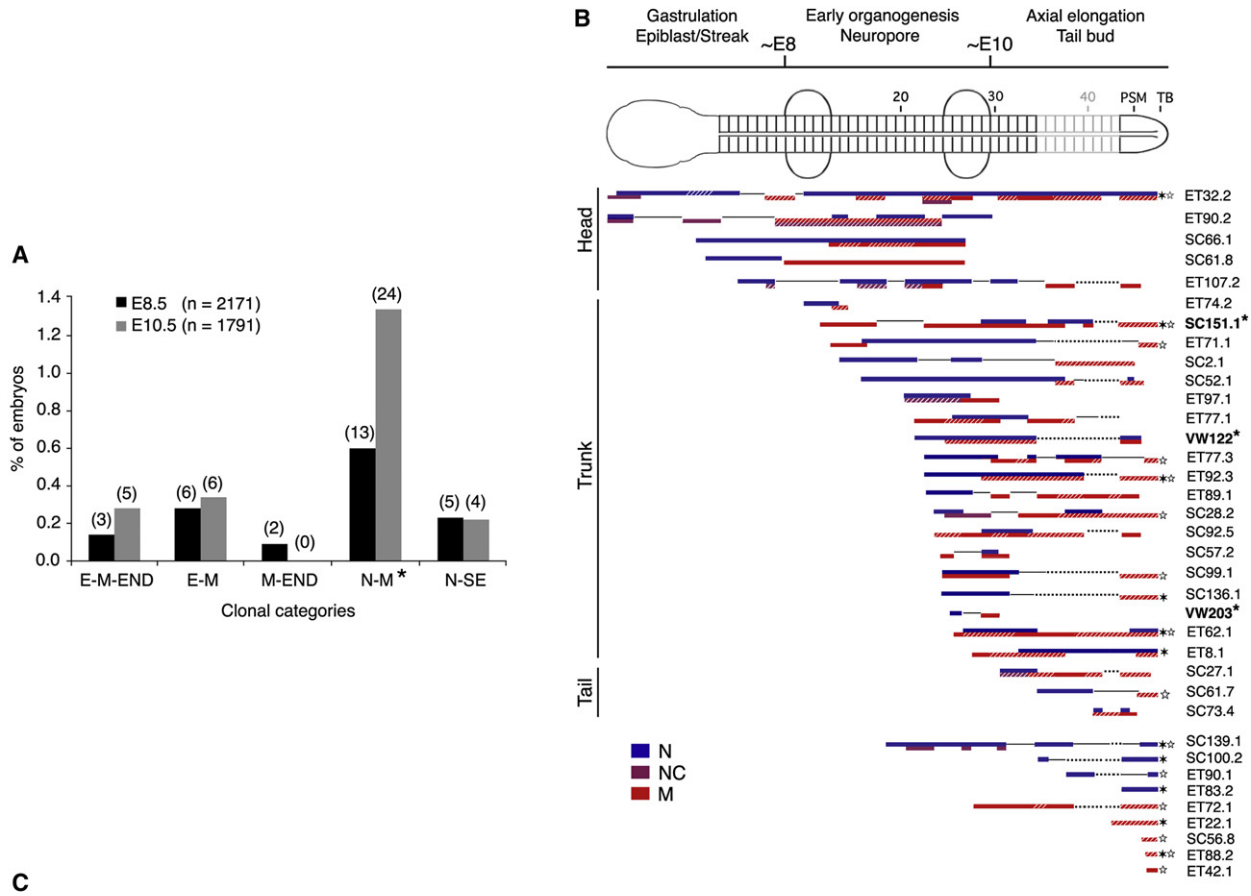
A
E8.5 (n = 2171)
E10.5 (n = 1791)
% of embryos
1.4
1.2
1.0
0.8
0.6
0.4
0.2
0.0
(3)
(5)
(6)
(6)
(2)
(0)
(13)
(24)
(5)
(4)
E-M-END
E-M
M-END
N-M *
N-SE
Clonal categories
B
Gastrulation
Epiblast/Streak
~E8
Early organogenesis
Neuropore
~E10
Axial elongation
Tail bud
20
30
40
PSM
TB
Head
Trunk
Tail
ET32.2
ET90.2
SC66.1
SC61.8
ET107.2
ET74.2
SC151.1*
ET71.1
SC2.1
SC52.1
ET97.1
ET77.1
VW122*
ET77.3
ET92.3
ET89.1
SC28.2
SC92.5
SC57.2
SC99.1
SC136.1
VW203*
ET62.1
ET8.1
SC27.1
SC61.7
SC73.4
SC139.1
SC100.2
ET90.1
ET83.2
ET72.1
ET22.1
SC56.8
ET88.2
ET42.1
N
NC
M
C
MB
HB
S
NT
S
ET32.2
HB
S
LPM
HL
LPM
NT
S
HL
SC66.1
S
NT
PSM/TBM
S
NT
ET71.1
NT
S
NT
S
ET74.2
PSM
S
NT
SC92.5
CNH
NT
SC100.2

a contribution restricted to these two tissues (12/19). The smallest neuromesodermal clone has only 24 cells located in the posterior nonsegmented part of the axis (Figure 4, AW6.1). These findings suggest that common progenitors for neural and mesodermal lineages (N-M) persist until at least late gastrulation (Figure 3B).

Common Neuromesodermal Progenitors Are Still Present in the Tail Bud

Since embryonic tissues form temporally in a rostrocaudal order, the anterior borders of nonrestricted clones are related to the period of embryogenesis during which the clones were born. It is therefore noteworthy that all nonrestricted clones with contribution to surface ectoderm and/or endoderm have an anterior border in the head and they either extend to the entire axis or are limited to the cranial and most anterior trunk regions formed during gastrulation (Figure 4, three upper clonal groups). In contrast, a prominent feature of N-M clones is that they extend from a variable anterior border up to the neuropore and all, except one, have descendants in the node/streak region where axial progenitors reside (Figure 4, lower clonal group; Cambray and Wilson, 2002, 2007). Additional small clones confined to the neuropore were also detected, some of which (n = 9, 1–8 cells) had labeled cells in the node/streak region (ectodermal component). These could contribute cell derivatives to the extending axis after this stage, if the embryos were allowed to develop further.

We therefore considered whether the clonal categories detected in E8.5 embryos can be traced forward to E10.5 embryos (35–43 somites), a stage at which the embryo has produced an additional 25 somites that constitute the posterior trunk and part of the tail. If progenitors of a given lineage segregate prior to E8.5, each category of nonrestricted clones contributing to this lineage will have similar frequencies at both stages. In contrast, if common progenitors for two or more lineages are still present after E8.5, we expect to obtain a higher frequency of clones in the corresponding categories at E10.5. Similar frequencies were found for the categories of clones contributing to all three germ layers, and those in tissue combinations including surface ectoderm or endoderm (Figure 5A). This finding further demonstrates that segregation of these tissue progenitors occurs before early organogenesis. In contrast, a significant increase was observed in the numbers of N-M clones between E8.5 and E10.5, suggesting a continued presence of common progenitors for these tissues (Figure 5A).

Nine E10.5 N-M clones have an anterior border at somite <16 and should therefore correspond to the labeling of progenitors concurrent to those that gave rise to E8.5 N-M clones (Figure 5B). From the additional 18 clones, restricted to more posterior axial levels, some may be equivalent to E8.5 streak clones, whereas remaining clones, in particular those in the tail, are most likely initiated after this stage and therefore have no E8.5 counterpart. The smallest tail N-M clone has only 25 cells (Figure 5B, SC73.4), suggesting a recent birth date, provided that a high proliferation rate is maintained in the progenitor region after early organogenesis. We compared the extent of BrdU incorporation in the streak to that in the emerging E9.5 tail bud. We found similar levels of BrdU incorporation at these stages (97%–98%; Figure S5), indicating that the progenitor population is still highly proliferative in the incipient tail bud. This is consistent with previous observations showing that the accelerated increase of axial length observed during this period is related to the rate of expansion of the progenitor population (Tam, 1981). Taken together, these data indicate that common N-M progenitors persist at tail bud stage.

A Major Rearrangement within the N-M Progenitor Pool

Examination of the axial patterns of E10.5 N-M clones ordered by their most anterior border allowed us to deduce the behavior of N-M progenitors during axis formation. Three main periods (gastrulation, early organogenesis, and tail bud stage), distinguished on the basis of changes in the morphogenetic processes and the progenitor population, correspond to subclasses of clones that we designate head, trunk, and tail clones, respectively (Figure 5B, examples in 5C). The overall distribution of clones exhibits posterior polarity, and the clonal complexity, defined as the number of times a given axial level is labeled by a clone, increases from anterior to posterior (Figure 6). These quantitative features describe the ability of N-M progenitors to produce differentiated derivatives colonizing increasingly more posterior levels of the elongating axis while maintaining cells in the progenitor region, and imply a self-renewing behavior of these cells. These characteristics were not observed in either neural or mesoderm-restricted R26nlaacZ clones that showed instead a uniform axial distribution (Figure S4 and data not shown).

Detailed inspection of the N-M axial patterns reveals certain differences between clonal subclasses. First, the number of clones with anterior border in the trunk is significantly higher compared to the other subclasses (n-head = 5, n-trunk = 19, n-tail = 3). Since the frequency of clones in each subclass is proportional to the number of progenitors at their origin, this points to an increase in the number of N-M progenitors between gastrulation and early organogenesis and a subsequent decrease during tail bud stage. Second, axial contribution

Figure 5. Common N-M Progenitors Persist after Gastrulation

(A) Percentage of *R26nlaacZ1.1* embryos at E8.5 and E10.5, presenting clones in each category out of the total embryos examined at each stage (n). The number of clones is shown in parenthesis. M, mesoderm; N, neurectoderm; SE, surface ectoderm; E, ectoderm (SE ± N); END, endoderm. Statistically significant difference between E8.5 and E10.5 frequencies is indicated by an asterisk (Fisher's exact test, p = 0.012).

(B) Schematic representation of N-M clones at E10.5. Tissues labeled are color coded as indicated. Contribution to specific mesodermal sublineages is omitted for clarity. Mesoderm labeling is exclusively paraxial in 16 of the 20 clones with anterior border > somite 12. Contribution to lateral mesoderm was more pronounced in head and anterior trunk clones (see also Figure 4). Other symbols are as in Figure 4. Asterisks represent labeled cells in different regions of the tail bud (filled asterisk, chordoneural hinge; open asterisk, tail bud mesoderm). Clone names in bold marked with a small asterisk correspond to R26nlaacZ0.3 clones. The last group of clones in the diagram colonize only neurectoderm or mesoderm but have cells in the tail bud and may therefore contribute descendants to both tissues after E10.5. N, neurectoderm; NC, neural crest; M, mesoderm.

(C) Examples of E10.5 N-M clones (lateral and dorsal views, anterior at the top except for the tails. CNH, chordoneural hinge; HB, hindbrain; HL, hindlimb; LPM, lateral plate mesoderm; NT, neural tube; S, somite; TBM, tail bud mesoderm; MB midbrain; PSM, presomitic mesoderm.

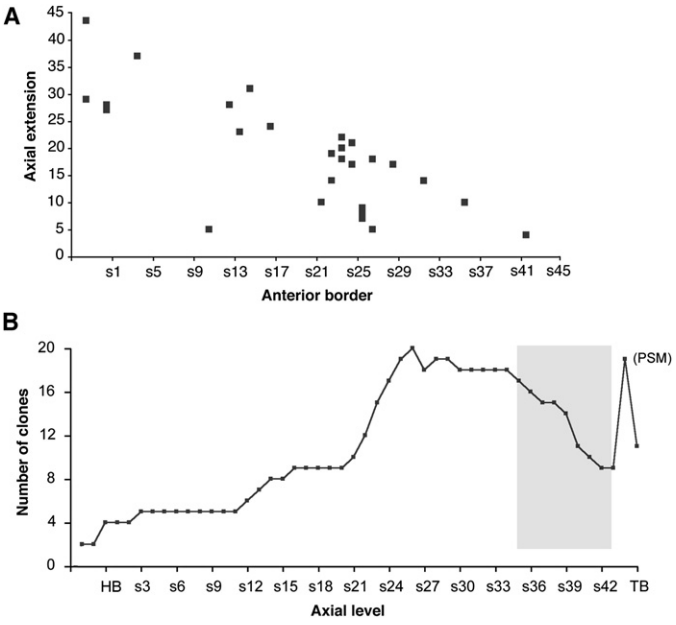

Figure 6. N-M Clones Are Derived from Self-Renewing Progenitors

(A) The axial extension of clones is inversely proportional to the position of their anterior border indicating that growth is polarized. The axial length is considered only for the postcranial axis and measured as number of somites. As a consequence, the length of head clones is slightly under represented.

(B) The number of clones contributing to each axial level (clonal complexity) increases from anterior to posterior. The area in gray corresponds to axial levels not formed in certain embryos due to age variation. HB, hindbrain; PSM, presomitic mesoderm; s1–42, somite levels; TB, tail bud.

arrests short of the tail in several of the clones (n = 6), reflecting their exit from the progenitor pool before tail bud stage. These differences raise the possibility that N-M subclasses derive from distinct progenitor pools.

To examine this possibility, we compared the actual distribution of N-M clones with the clonal patterns predicted by the two main temporal models for the organization of progenitor cells (Eloy-Trinquet et al., 2000; Nicolas et al., 1996; Figure 7). According to model A, all N-M clones derive from progenitors organized into a genealogically coherent pool of cells before initiation of axial elongation. Descendants of N-M founder cells are maintained in the pool by self-renewal and produce derivatives that sequentially exit to the elongating axis and differentiate. Since a single pool operates during the entire period of axis elongation, there is clonal continuity between all axial levels. In contrast, according to model B, two distinct pools of N-M progenitors function successively during axis elongation. Thus, the longest N-M clones produced by the founder cells of each of these pools would contribute only to a fraction of the axis, such that there is no clonal continuity between anterior and posterior axial levels. The third case depicted in Figure 7 shows a simplified representation of the actual N-M patterns observed (Figure 5B). Their distribution presents similarities but also differences with both models. However, the existence of N-M clones contributing to all or most axial levels from head to tail (Figure 5B, ET32.2, ET107.2) strongly supports that the N-M subclasses derive from a single N-M pool present from gastrulation to tail bud stage. The divergence from model A seems to concern the behavior of progenitors after constitution of the pool. Specifically, the simplified arrangement of clones emphasizes that the arrest of axial contribution of most head and few trunk clones coincides with a prominent increase in the number of trunk clones. This observation suggests a major re-arrangement within the pool with depletion of a significant proportion of early-pool descendants and concomitant expansion of a subpopulation of cells that mainly contributes to posterior axial levels.

DISCUSSION

We have used retrospective analysis of ubiquitous *laacZ/lacZ* revertant clones to examine the progression of lineage segregations during establishment of the mouse anteroposterior axis. Our results demonstrate that common neuromesodermal progenitors persist long after segregation of endoderm and surface ectoderm lineages, which occurs before the end of gastrulation. Following posterior neuropore closure (~26 somite stage), these N-M progenitors are incorporated in the tail bud where they continue to supply descendants to both tissues in the tail.

Hierarchy of Cell Fate Choices: Germ Layers and Specific Tissues

The conventional view of vertebrate development holds that the three germ layers, formed by gastrulation, are key intermediates in differentiation of the pluripotent primordium toward tissue-specific precursors. This idea has influenced the strategies developed for differentiation of ES cells toward specific tissue lineages in vitro. Our results challenge this view showing that, at least in mouse, there is a closer genealogical relationship between neurectoderm and mesoderm than between the two ectodermal lineages (surface and neural ectoderm). This would imply that the germ layer concept has a morphological, location-based rather than a lineage-based significance.

Related to this idea, the term mesendoderm has often been employed to designate an intermediate germ layer from which embryonic endoderm and mesoderm subsequently segregate (Lewis and Tam, 2006; Rodaway and Patient, 2001). In zebrafish, prospective endoderm and mesoderm cells remain intermingled in the hypoblast until early segmentation (Kimmel et al., 1995), and lineage tracing indicates that single cells in the late blastula can contribute derivatives to both lineages (Warga and Nusslein-Volhard, 1999). However, evidence for such bipotent progenitors of a distinct mesendodermal layer in mouse is missing. Indeed, a recent study by Burtscher and Lickert (2009) shows that T and Foxa2, which are upregulated in prospective mesoderm and endoderm respectively, are mutually exclusive in the pre-streak epiblast, suggesting that at least some segregation of endoderm from the bulk of mesoderm may occur before cell delamination in the early streak. On the other hand, single cell fate maps show that endoderm derives from a region of the early gastrulation epiblast that generates the highest frequency of clones with multiple tissue contribution, including neurectoderm (Lawson et al., 1991). The clonal patterns observed in *R26nlaacZ*

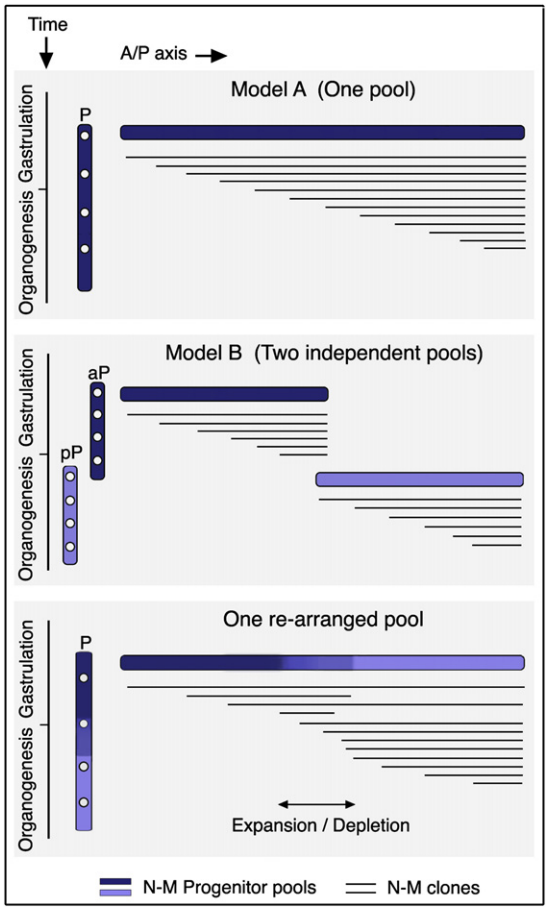

Figure 7. A Self-Sustained N-M Progenitor Pool Functions from Gastrulation to Tail Bud Stage

Top panels: models for the organization of N-M progenitors with respect to their axial contribution. Each thin horizontal line corresponds to a single clone initiated at the time indicated on the vertical axis. Model A: a single N-M pool (P) is present throughout axial elongation. *LaacZ* recombination in a cell within the pool gives rise to a clone extending from a variable anterior level, depending on the stage during elongation that the clone was initiated, to the caudal end of the embryo. The longest clones, initiated in founder cells of the pool, contribute to all axial levels. Model B: anterior and posterior levels are formed by two independent progenitor pools, aP and pP, respectively, such that there is no clonal continuity between these parts of the axis. The longest clones initiated in each of the pools contributes only to a fraction of the axis. Bottom panel: simplified representation of the distribution of N-M clonal patterns in Figure 5B. The presence of N-M clones with contribution to all axial levels (from head to tail) indicates a clonal continuity in the axis, as predicted by model A. The arrest of contribution of several clones in axial levels formed during early organogenesis and the concurrent increase of the number of clones with anterior border in this region would result from a rearrangement within the pool during this stage.

embryos indicate a closer relationship between endoderm and early ingressing mesodermal cell types (heart and extraembryonic) than between endoderm and ectoderm or more posterior mesoderm. However, the early segregation of endoderm from other lineages, including anterior mesoderm, and the low number of ''mesendoderm'' clones (Figure 5A), do not support the existence of an obligate mesendoderm-specific progenitor. This does not rule out the possibility that a similar set of factors may influence allocation of cells to endoderm and specific mesodermal sublineages. It is also noteworthy that contrary to the initial view that definitive endoderm derives exclusively from the epiblast, a recent study by Kwon et al. (2008) shows contribution of visceral endoderm to the embryonic gut, suggesting that differentiation to definitive endoderm may be possible via very diverse routes.

Putative Locations of the N-M Progenitor Pool during Axial Elongation

Previous retrospective clonal analyses of the mouse spinal cord and embryonic muscle, using tissue-specific laacZ approaches, indicated that these tissues derive from pool(s) of stem cell progenitors. These give rise to long clones (>6 somites) whose distribution presents posterior polarity and posteriorly increasing clonal complexity (Mathis and Nicolas, 2000; Nicolas et al., 1996). The ubiquitous laacZ approach employed here revealed that the only clonal category with similar characteristics is that of N-M clones. In contrast, neural or mesoderm-restricted R26nlaacZ clones are shorter and uniformly distributed along the axis, suggesting that these derive from transient, probably committed precursors.

Fate mapping studies have suggested locations for long-term axial progenitors contributing to neural tube and mesoderm in mouse and chick. These correspond to the node-streak border and the epiblast lateral to the primitive streak at E8.5 (2–6 somites; Cambray and Wilson, 2007; McGrew et al., 2008). Some descendants of cells in these locations are retained in the CNH at E10.5, the only tail bud region displaying stem cell-like properties upon serial transplantation (Cambray and Wilson, 2002; McGrew et al., 2008). Therefore, most likely, bipotent progenitors at the origin of N-M R26nlaacZ clones are located successively in these regions during axis elongation. Interestingly, the midline E8.5 primitive streak is exclusively mesodermal in fate and does not contribute to the CNH of the tail bud, suggesting that these cells are mesoderm-restricted progenitors with more limited axial contribution (Cambray and Wilson, 2007). Thus, at least some of the R26nlaacZ short mesoderm-restricted clones may have originated in this latter location. Contrary to the fate mapping studies mentioned above, made by grafting of cells stably expressing a ubiquitous GFP reporter, polyclones generated by DiI injection to groups of up to three cells in the chick caudal neural plate at HH stage 6 (mouse ~E8) never extended as far as the tail bud, but instead contributed only to short axial segments (Brown and Storey, 2000). This suggests that stem cells, at least in chick at this stage, are outnumbered by transient precursors, or alternatively, the absence of long clones in this latter study may be due to dilution of dye following multiple cell divisions.

Bipotent Self-Renewing N-M Progenitors and the Control of Axial Elongation

The existence of a permanent pool of bipotent N-M cells provides new insight on lineage diversification, suggesting that the initial steps leading to differentiation of these tissues may be regulated and coordinated by the same genetic pathways during the entire period of axis elongation. Indeed, gene expression studies revealed coexpression of early neural and mesodermal markers in the streak and tail bud of mouse and chick

(Cambray and Wilson, 2007; Delfino-Machin et al., 2005; Iimura et al., 2007). In addition, null mutations of *FGFR1, Wnt3a* and downstream effectors *T*, *Tbx6* and *Lef1*/*Tcf1* lead to axial truncations associated with ectopic formation of neurectoderm at the expense of mesoderm (Beddington et al., 1992; Chapman and Papaioannou, 1998; Ciruna et al., 1997; Galceran et al., 2001; Takada et al., 1994; Wilson and Beddington, 1996; Yamaguchi et al., 1999). Variable T protein levels were observed in individual streak cells of wild-type E7.5 embryos, and manipulation of T levels in chimeras showed that cells expressing low T levels tend to differentiate into neural tissue, while those expressing high levels exit rapidly from the streak to mesoderm (Wilson and Beddington, 1997). Opposite effects in the production of neural and mesodermal tissues were also seen upon manipulation of FGF signaling in chick embryos (Diez del Corral et al., 2002; Mathis et al., 2001). Furthermore, a direct correlation was found between gene expression levels and the extent of axial truncation, as indicated by the less severe phenotypes of hypomorph mutants or heterozygotes of *Wnt3a*, *FGFR1*, and *T* (Beddington et al., 1992; Greco et al., 1996; Partanen et al., 1998). Accordingly, FGFR1 and T were shown to affect the maintenance of cells in the progenitor region. While downregulation of FGFR1 results in premature exit of cells from the progenitor pool, absence of T causes ectopic accumulation of cells in the streak and tail bud (Mathis et al., 2001; Wilson and Beddington, 1997). Thus, a tight regulation of Wnt and FGF cascades in axial progenitors seems critical both for proper allocation of their derivatives to neural and mesodermal tissues, and maintenance of the progenitor pool. We propose that these genes function within the N-M pool in a dose-dependent manner to finely tune maintenance of the bipotent N-M state and N or M fate decisions and thus ensure a balance between sustained axial elongation and coordinated neural and mesodermal differentiation.

Expansion and Depletion of Cells within the N-M Pool

The increase in the frequency of N-M clones in axial levels formed after gastrulation indicates an overall expansion of the N-M pool size during early organogenesis (Figure 5B). However, this expansion coincides with an exit of cells from the pool as suggested by the arrest of several clones at the posterior trunk level. This raises the possibility that the composition of the N-M pool evolves over the period of axis elongation. Interestingly, this pool rearrangement takes place during formation of the axial region where truncation occurs in most of the null mutants mentioned above. Although it is not yet clear whether early-depleted N-M progenitors have different characteristics from the expanding progenitor population, it is tempting to speculate that these genes play a major role in maintenance of the late N-M pool. This could explain the fact that mutations in genes such as *T*, expressed from early gastrulation onward, affect only the development of axial levels posterior to the forelimb bud (Beddington et al., 1992).

A large proportion of the clones that extend to the tail do not have descendants in the tail bud, suggesting a further depletion of progenitors toward the end of axial elongation. This depletion is concurrent with a decrease in expression of genes required for continued axis elongation within the tail bud from E10 onward (Cambray and Wilson, 2007 and unpublished data) and may be the underlying cause for the cessation of axis elongation around E13.

EXPERIMENTAL PROCEDURES

Production and Functional Testing of *R26nlaacZ* ES Cell Lines

The inactive *nlaacZ0.3* and *nlaacZ1.1* reporters, described previously (Bonnerot and Nicolas, 1993; Meilhac et al., 2003), and the control *nlacZ* reporter were each inserted into XhoI-linearized pBigT vector (Srinivas et al., 2001). An AscI-PacI fragment of the resulting construct, carrying the reporter cDNA downstream of a splice acceptor and a PGK-neomycin^R-pA cassette flanked by loxP sites, was subcloned into pRosa26PA vector (Srinivas et al., 2001) carrying Rosa26 homology arms. The resulting R26pAnlaacZ0.3, R26pAnlaacZ1.1, and control R26pAnlacZ targeting constructs were KpnI-linearized and electroporated into E14TG2a ES cells as described (Tzouanacou et al., 2003). Targeted neo-resistant colonies were transiently transfected with pCAGGS-Cre-IRESpuro vector and duplicates of neo-sensitive colonies were screened by Southern blot to verify excision of the floxed PGK-neomycin^R-pA cassette. The in vitro rate of *nlaacZ* intragenic recombination per cell and per generation was determined in the Cre-excised *R26nlaacZ* ES cell lines by fluctuation analysis (Bonnerot and Nicolas, 1993; Luria and Delbrück, 1943).

Mice

Chimeric males, produced by injection of the initial (nonexcised) *R26pAnlaacZ0.3*/*1.1* and control *R26pAnlacZ* ES cells into C57BL/6 host blastocysts, were mated to C57BL/6 females. F1 heterozygotes were crossed to a Cre-deleter line (*PGK-Cre*) to excise the PGK-*neomycin*^{R}-pA cassette. Offspring carrying the targeted Cre-excised alleles were detected by Southern blot and backcrossed for five generations to C57BL/6 mice before generating homozygote *R26nlaacZ* and *R26nlacZ* (*Cre*$^{-/-}$) lines by intercross.

Production and Description of Clones

Embryos produced by mating homozygotes *R26nlaacZ* males to wild-type (C57BL/6xDBA/2 or MF1) females or by homozygote intercross (*R26nlaacZ0.3*) were recovered between 13.00 and 16.00 hr at various embryonic stages. Noon of the day when the vaginal plug was found was considered E0.5. Embryos were stained with X-gal as described (Nicolas et al., 1996). Clones were observed under a Leica MZ16 stereomicroscope and photographed using Leica DFC320R2 camera and Openlab v5.1 software. Clonal parameters were recorded by observation of whole-mount embryos and confirmed in cryosections (7–10 μm).

Estimation of Growth Rate between E6.5 and E8.5

For cells dividing exponentially, the growth rate during the time interval $t - t_0$ is $r = (t - t_0)/n$, where n is the number of divisions. n can be calculated from $N = N_0 2^n$ with N and N_0 the number of cells at time points t and t_0, respectively. To determine the number of cells at E8.5, embryos (8–10 somites) were dissected from the yolk sac, and single cell suspensions were obtained from pools of 2–3 embryos using either 2.5% trypsin-EDTA (Palis et al., 1999) or 60% glacial acetic acid (3:1 ethanol/glacial acetic acid) in fixed embryos (Burns and Hassan, 2001). Both protocols gave similar cell counts. Cell suspensions were examined under an inverted microscope and cell number (mean of 5 counts ± SEM) was determined using an hemocytometer. The number of cells in E6.5 and E7.5 embryos was previously reported (Snow, 1977).

BrdU Cell Proliferation Analysis

E7.5 to E8.5 embryos and E9.5 tail pieces (MF1) were cultured in the presence of BrdU (BD PharMingen) for 5 hr as described (Bellomo et al., 1996). Culture conditions were as in Cockroft (1990). At the end of the culture, embryos were fixed overnight in 4% PFA, cryosectioned, and stained with α-BrdU (Roche) according to manufacturer's instructions. Percentages of labeled cells in E7.5–E8 primitive streak, E8.5 posterior neuropore and E9.5 tail bud were determined by cell counts in ≥11 sections of ≥3 embryos at each stage.

Statistical Analysis of Clonality

Reversion of *nlaacZ* to *nlacZ* by homologous intragenic recombination is a spontaneous random event (Bonnerot and Nicolas, 1993). The frequency of its occurrence can therefore be analyzed using the fluctuation test of Luria and Delbrück (1943). The number of independent recombinations that have occurred during embryo growth follows a Poisson distribution with parameter

aNt (a, in vivo rate of recombination; Nt, total number of cells in the embryo). The in vivo rate (a) can be estimated by $-\ln(p_0)/Nt$ (p_0, fraction of negative embryos) and the parameter of the Poisson distribution by $-\ln(p_0)$. The expected number of embryos presenting k independent recombination events is $E_0(\ln(E_{ex}/E_0))^k/(k!)$, with E_0 the number of negative embryos and E_{ex} the total embryos examined at the stage considered.

Other Statistical Analysis

The frequencies of clonal categories correspond to the percentage of embryos showing clones in each category out of the total embryos examined (labeled and unlabeled) at each embryonic stage unless otherwise stated. Statistical significance of differences between observed and expected frequencies was assessed by Fisher's exact test. Curve fitting in Figure 2A′ was performed by regression analysis. EXCEL software was used.

SUPPLEMENTAL DATA

Supplemental Data include five figures, two tables, and supplemental text and can be found with this article online at http://www.cell.com/developmental-cell/supplemental/S1534-5807(09)00339-6.

ACKNOWLEDGMENTS

We thank P. Avner, M. Buckingham, E. Hirsinger, T. Kunath, K. Lawson, AG. Smith, and S. Tajbakhsh for helpful comments on the manuscript; S. Capgras, R. Wilkie, and J. Beaton for technical assistance; S. Meilhac, A.J.H. Smith, and P. Brûlet for providing materials. Support was provided by the EU FP6 (''EuroStemCell'' Integrated Project, JDRF/EuroStemCell Bridge funds, ''Cells into Organs'' Network of Excellence, Marie-Curie IE Fellowship to E.T.), the Institut Pasteur and the BBSRC. J-.F.N. is an INSERM Investigator.

Received: February 2, 2009
Revised: June 24, 2009
Accepted: August 11, 2009
Published: September 14, 2009

REFERENCES

Beddington, R.S., Rashbass, P., and Wilson, V. (1992). Brachyury—a gene affecting mouse gastrulation and early organogenesis. Dev. Suppl., 157–165.

Bellomo, D., Lander, A., Harragan, I., and Brown, N.A. (1996). Cell proliferation in mammalian gastrulation: the ventral node and notochord are relatively quiescent. Dev. Dyn. *205*, 471–485.

Bonnerot, C., and Nicolas, J.F. (1993). Clonal analysis in the intact mouse embryo by intragenic homologous recombination. C. R. Acad. Sci. III *316*, 1207–1217.

Brown, J.M., and Storey, K.G. (2000). A region of the vertebrate neural plate in which neighbouring cells can adopt neural or epidermal fates. Curr. Biol. *10*, 869–872.

Burns, J.L., and Hassan, A.B. (2001). Cell survival and proliferation are modified by insulin-like growth factor 2 between days 9 and 10 of mouse gestation. Development *128*, 3819–3830.

Burtscher, I., and Lickert, H. (2009). Foxa2 regulates polarity and epithelialization in the endoderm germ layer of the mouse embryo. Development *136*, 1029–1038.

Cambray, N., and Wilson, V. (2002). Axial progenitors with extensive potency are localised to the mouse chordoneural hinge. Development *129*, 4855–4866.

Cambray, N., and Wilson, V. (2007). Two distinct sources from a population of maturing axial progenitors. Development *134*, 2829–2840.

Chapman, D.L., and Papaioannou, V.E. (1998). Three neural tubes in mouse embryos with mutations in the T-box gene Tbx6. Nature *391*, 695–697.

Ciruna, B.G., Schwartz, L., Harpal, K., Yamaguchi, T.P., and Rossant, J. (1997). Chimeric analysis of fibroblast growth factor receptor-1 (Fgfr1) function: a role for FGFR1 in morphogenetic movement through the primitive streak. Development *124*, 2829–2841.

Cockroft, D.L. (1990). Dissection and culture of post-implantation embryos. In Postimplantation Mammalian Embryos A practical Approach, A.J. Coop and D.L. Cockroft, eds. (Oxford: Oxford University Press), pp. 15–39.

Delfino-Machin, M., Lunn, J.S., Breitkreuz, D.N., Akai, J., and Storey, K.G. (2005). Specification and maintenance of the spinal cord stem zone. Development *132*, 4273–4283.

Diez del Corral, R., Breitkreuz, D.N., and Storey, K.G. (2002). Onset of neuronal differentiation is regulated by paraxial mesoderm and requires attenuation of FGF signalling. Development *129*, 1681–1691.

Eloy-Trinquet, S., and Nicolas, J.F. (2002a). Cell coherence during production of the presomitic mesoderm and somitogenesis in the mouse embryo. Development *129*, 3609–3619.

Eloy-Trinquet, S., and Nicolas, J.F. (2002b). Clonal separation and regionalisation during formation of the medial and lateral myotomes in the mouse embryo. Development *129*, 111–122.

Eloy-Trinquet, S., Mathis, L., and Nicolas, J.F. (2000). Retrospective tracing of the developmental lineage of the mouse myotome. Curr. Top. Dev. Biol. *47*, 33–80.

Galceran, J., Hsu, S.C., and Grosschedl, R. (2001). Rescue of a Wnt mutation by an activated form of LEF-1: regulation of maintenance but not initiation of Brachyury expression. Proc. Natl. Acad. Sci. USA *98*, 8668–8673.

Gardner, R.L., and Rossant, J. (1979). Investigation of the fate of 4-5 day post-coitum mouse inner cell mass cells by blastocyst injection. J. Embryol. Exp. Morphol. *52*, 141–152.

Greco, T.L., Takada, S., Newhouse, M.M., McMahon, J.A., McMahon, A.P., and Camper, S.A. (1996). Analysis of the vestigial tail mutation demonstrates that Wnt-3a gene dosage regulates mouse axial development. Genes Dev. *10*, 313–324.

Griffith, C.M., Wiley, M.J., and Sanders, E.J. (1992). The vertebrate tail bud: three germ layers from one tissue. Anat. Embryol. (Berl.) *185*, 101–113.

Handrigan, G.R. (2003). Concordia discors: duality in the origin of the vertebrate tail. J. Anat. *202*, 255–267.

Iimura, T., Yang, X., Weijer, C.J., and Pourquie, O. (2007). Dual mode of paraxial mesoderm formation during chick gastrulation. Proc. Natl. Acad. Sci. USA *104*, 2744–2749.

Kimmel, C.B., Ballard, W.W., Kimmel, S.R., Ullmann, B., and Schilling, T.F. (1995). Stages of embryonic development of the zebrafish. Dev. Dyn. *203*, 253–310.

Kwon, G.S., Viotti, M., and Hadjantonakis, A.K. (2008). The endoderm of the mouse embryo arises by dynamic widespread intercalation of embryonic and extraembryonic lineages. Dev. Cell *15*, 509–520.

Lawson, K.A., and Pedersen, R.A. (1992). Clonal analysis of cell fate during gastrulation and early neurulation in the mouse. Ciba Found. Symp. *165*, 3–21.

Lawson, K.A., Meneses, J.J., and Pedersen, R.A. (1991). Clonal analysis of epiblast fate during germ layer formation in the mouse embryo. Development *113*, 891–911.

Lewis, S.L., and Tam, P.P. (2006). Definitive endoderm of the mouse embryo: formation, cell fates, and morphogenetic function. Dev. Dyn. *235*, 2315–2329.

Luria, S.E., and Delbrück, M. (1943). Mutations of bacteria from virus sensitivity to virus resistance. Genetics *28*, 491–511.

Mathis, L., and Nicolas, J.F. (2000). Different clonal dispersion in the rostral and caudal mouse central nervous system. Development *127*, 1277–1290.

Mathis, L., and Nicolas, J.F. (2003). Progressive restriction of cell fates in relation to neuroepithelial cell mingling in the mouse cerebellum. Dev. Biol. *258*, 20–31.

Mathis, L., and Nicolas, J.F. (2006). Clonal origin of the mammalian forebrain from widespread oriented mixing of early regionalized neuroepithelium precursors. Dev. Biol. *293*, 53–63.

Mathis, L., Kulesa, P.M., and Fraser, S.E. (2001). FGF receptor signalling is required to maintain neural progenitors during Hensen's node progression. Nat. Cell Biol. *3*, 559–566.

McGrew, M.J., Sherman, A., Lillico, S.G., Ellard, F.M., Radcliffe, P.A., Gilhooley, H.J., Mitrophanous, K.A., Cambray, N., Wilson, V., and Sang, H. (2008).

Localised axial progenitor cell populations in the avian tail bud are not committed to a posterior Hox identity. Development *135*, 2289–2299.

Meilhac, S.M., Kelly, R.G., Rocancourt, D., Eloy-Trinquet, S., Nicolas, J.F., and Buckingham, M.E. (2003). A retrospective clonal analysis of the myocardium reveals two phases of clonal growth in the developing mouse heart. Development *130*, 3877–3889.

Meilhac, S.M., Esner, M., Kelly, R.G., Nicolas, J.F., and Buckingham, M.E. (2004a). The clonal origin of myocardial cells in different regions of the embryonic mouse heart. Dev. Cell *6*, 685–698.

Meilhac, S.M., Esner, M., Kerszberg, M., Moss, J.E., and Buckingham, M.E. (2004b). Oriented clonal cell growth in the developing mouse myocardium underlies cardiac morphogenesis. J. Cell Biol. *164*, 97–109.

Nicolas, J.F., Mathis, L., and Bonnerot, C. (1996). Evidence in the mouse for self-renewing stem cells in the formation of a segmented longitudinal structure, the myotome. Development *122*, 2933–2946.

Palis, J., Robertson, S., Kennedy, M., Wall, C., and Keller, G. (1999). Development of erythroid and myeloid progenitors in the yolk sac and embryo proper of the mouse. Development *126*, 5073–5084.

Partanen, J., Schwartz, L., and Rossant, J. (1998). Opposite phenotypes of hypomorphic and Y766 phosphorylation site mutations reveal a function for Fgfr1 in anteroposterior patterning of mouse embryos. Genes Dev. *12*, 2332–2344.

Rodaway, A., and Patient, R. (2001). Mesendoderm. an ancient germ layer? Cell *105*, 169–172.

Schoenwolf, G.C. (1984). Histological and ultrastructural studies of secondary neurulation in mouse embryos. Am. J. Anat. *169*, 361–376.

Schoenwolf, G.C., and Delongo, J. (1980). Ultrastructure of secondary neurulation in the chick embryo. Am. J. Anat. *158*, 43–63.

Snow, M.H.L. (1977). Gastrulation in the mouse: growth and regionalization of the epiblast. J. Embryol. Exp. Morphol. *42*, 293–303.

Soriano, P. (1999). Generalized lacZ expression with the ROSA26 Cre reporter strain. Nat. Genet. *21*, 70–71.

Srinivas, S., Watanabe, T., Lin, C.S., William, C.M., Tanabe, Y., Jessell, T.M., and Costantini, F. (2001). Cre reporter strains produced by targeted insertion of EYFP and ECFP into the ROSA26 locus. BMC Dev. Biol. *1*, 4.

Stern, C.D., Charite, J., Deschamps, J., Duboule, D., Durston, A.J., Kmita, M., Nicolas, J.F., Palmeirim, I., Smith, J.C., and Wolpert, L. (2006). Head-tail patterning of the vertebrate embryo: one, two or many unresolved problems? Int. J. Dev. Biol. *50*, 3–15.

Takada, S., Stark, K.L., Shea, M.J., Vassileva, G., McMahon, J.A., and McMahon, A.P. (1994). Wnt-3a regulates somite and tail bud formation in the mouse embryo. Genes Dev. *8*, 174–189.

Tam, P.P.L. (1981). The control of somitogenesis in mouse embryos. J. Embryol. Exp. Morphol. *65* (*Suppl*), 103–128.

Tam, P.P.L., and Beddington, R.S.P. (1987). The formation of mesodermal tissues in the mouse embryo during gastrulation and early organogenesis. Development *99*, 109–126.

Tam, P.P.L., and Behringer, R.R. (1997). Mouse gastrulation: the formation of a mammalian body plan. Mech. Dev. *68*, 3–25.

Tzouanacou, E., Tweedie, S., and Wilson, V. (2003). Identification of Jade1, a gene encoding a PHD zinc finger protein, in a gene trap mutagenesis screen for genes involved in anteroposterior axis development. Mol. Cell. Biol. *23*, 8553–8562.

Warga, R.M., and Nusslein-Volhard, C. (1999). Origin and development of the zebrafish endoderm. Development *126*, 827–838.

Wilkie, A.L., Jordan, S.A., and Jackson, I.J. (2002). Neural crest progenitors of the melanocyte lineage: coat colour patterns revisited. Development *129*, 3349–3357.

Wilson, V., and Beddington, R.S. (1996). Cell fate and morphogenetic movement in the late mouse primitive streak. Mech. Dev. *55*, 79–89.

Wilson, V., and Beddington, R. (1997). Expression of T protein in the primitive streak is necessary and sufficient for posterior mesoderm movement and somite differentiation. Dev. Biol. *192*, 45–58.

Yamaguchi, T.P., Takada, S., Yoshikawa, Y., Wu, N., and McMahon, A.P. (1999). T (Brachyury) is a direct target of Wnt3a during paraxial mesoderm specification. Genes Dev. *13*, 3185–3190.